International Journal on Engineering, Science and Technology
Volume 4, Issue 1, 2022 ISSN: 2642-4088

Numerical Investigation of Performance of Continuous Composite Girders with UHPC slab at Hogging Moment

Nizar A. Assi
Department of Civil Engineering, Birzeit University, Birzeit, Palestine, naassi@birzeit.edu

Abstract: This paper intends to investigate the behavior of continuous composite girders with of ultra-high-performance concrete (UHPC) slab at hogging moment zone utilizing the nonlinear finite element (FE) modeling. A nonlinear three-dimensional FE model of the continuous composite girder was developed utilizing the commercial software ABAQUS. The model considers both material and geometric nonlinearities. Behavior of normal concrete (NC) and UHPC was modeled utilizing damage plasticity model. Tied, normal & friction behavior, embedded contacts were used to simulate the interfacial zones between contacted elements. Four different models were developed and validated with experimental results. The verified model showed satisfactory behavior and is capable of predicting the loading history for continuous composite girders. The model can capture the modes of failure either in normal concrete slab at sagging moment zone or delaminating of UHPC layer at hogging moment zone. A parametric study was carried out to investigate the effect of length of UHPC slab at hogging moment zone on the behavior of the continuous composite girders. The findings of the parametric study showed that the length of UHPC slab slightly affects the ultimate capacity, yielding load, and stiffness of the composite girders. However, significant enhancement in cracking loads was obtained as increasing the length of UHPC slab.

Keywords: Ultra-high-performance concrete (UHPC), Composite action, Two-span composite girders, Structural strengthening, finite element model

Introduction

The concrete slab at the hogging moment zone of continuous composite steel-concrete girders subjects to tension and consequently loses its contribution to the composite action. The American Institute of Steel Construction (AISC) [1] code ignores the contribution of concrete slab at hogging moment zone for continuous composite girders or considers the steel reinforcements of concrete slab to act compositely with steel section. For both options of AISC code, the section capacity at hogging moment zone greatly reduced.

Researchers tried different schemes to improve the capacity of the composite action at the hogging moment zone for continuous composite girders. Experimental and analytical investigation on the use of prestressing technique was used by several investigators to enhance the capacity of composite girders Basu et al. [2, 3], Elremaily and Yehia [4], Chen et al. [5], Nie et al. [6]. Carbon fibre–reinforced polymer (CFRP) was used at hogging moment zone of continuous composite girders to maintain the composite action at the hogging moment zone. Sharif el al. (2016) [7] conducted experimental investigation on the use of CFRP to maintain the composite action at hogging moment zone. Samaaneh et al. (2016) [8] conducted numerical investigation of two-span, continuous composite steel-concrete girders strengthened with CFRP utilizing ABAQUS software. The results obtained from the model were validated with experimental results Sharif et al. [7].

The results demonstrated that the thickness of CFRP sheet depends on adhesive strength and the capacity of the girder at sagging moment. Steel fiber-reinforced concrete technique was used by Lin el al. [9, 10] to investigate the mechanical properties of composite steel concrete girders under hogging moment. Inverted simply supported beams were tested to study the effect of steel fiber-reinforced concrete on the behavior of the composite girders. Experimental and numerical investigations were conducted and it was shown that the current AASHTO and LRFD [11] specifications underestimate the plastic bending moment. In addition, steel fiber-reinforced concrete controls the cracks.

A review of the published research has not shown a lot of experiment or numerical works on the use ultra-high-performance concrete (UHPC) slab at hogging moment zone for continuous composite girders. Therefore, the purpose of this study is to investigate numerically in detail the effect of the length of UHPC slab on the performance of a two-span continuous composite steel-concrete girders at hogging moment zone. Therefore, a 3-dimensional FE model was developed for a two-span continuous composite girder. The developed FE model was validated with the obtained experimental results [12]. Different FE models were developed to study the

behavior of the composite girders with different length of UHPC slab at hogging moment zone. A half-depth UHPC slab thickness and a 50%-degree of shear connection, as suggested by Sharif experimentally [12], were implemented at hogging moment zone to evaluate the proper UHPC slab length that is sufficient for all loading conditions.

Geometrical and Material Properties

Finite element modeling utilizing ABAQUS software [13] was performed for particular geometrical and material properties of two-span continuous composite girders. Those properties were identified to be identical to the properties of the experimentally tested girders [12] to validate the developed FE models. The geometrical properties of the composite girders including sectional and side views, rebar, thickness of concrete slabs, and studs spacing are shown in Figure 1 to Figure 3. Studs spacing and NC slab at sagging moment zone were identical for all girders. Whereas, the thickness of UHPC slab and stud spacing were varied at hogging moment zone as given in Table 1. For the material properties, all materials incorporated in the composite girder were tested experimentally [12] according to ASTM standard methods [14, 15, and 16].

Mechanical properties of NC, UHPC, steel beam, and rebar were evaluated and given by Table 2 and Table 3. UHPC mix proportions was developed and proposed by Hakeem [17]. In addition, stress-strain curves of all materials under compression and tension were identified and shown in Figure 4 to Figure 9. Moreover, the capacity, 151.3 kN, of a 19 mm-diameter shear stud at hogging moment zone was evaluated experimentally [12] according to Eurocode 4 [18]. While, capacity of shear studs within sagging moment zones was evaluated [12] using AISC specification. Regarding testing of the two-span continuous composite girders, they were tested and investigated under monotonic loads applied on each span up to flexural failure. Local failure in steel beam was avoided by satisfying width to thickness ratio of flanges and web, lateral-torsional buckling was prevented by lateral support provided for the compression flange over interior support.

In this study, four FE models were developed using ABAQUS software and validated against the experimental results [12]. Mechanical properties and stress strain curves of materials were used as input parameters for the FE modeling. The verified model was used to study the effect of the length of UHPC slab at hogging moment zone onto the behavior of continuous composite girders.

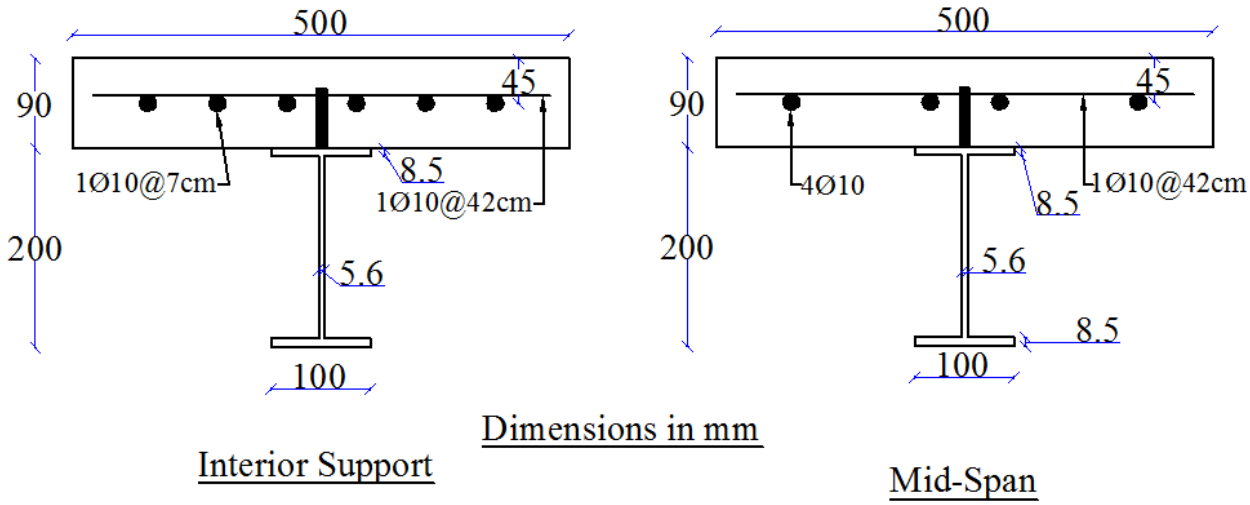

Figure 1. Girder's Cross Sections at both Mid-span and İnterior Support

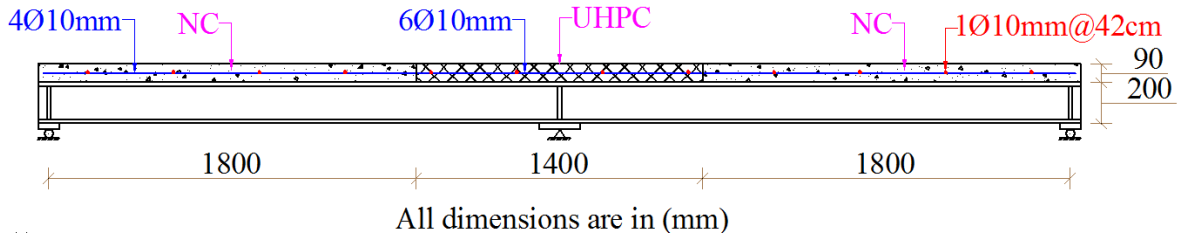

Figure 2. Detailed Dimensions of the Fabricated Composite Girder

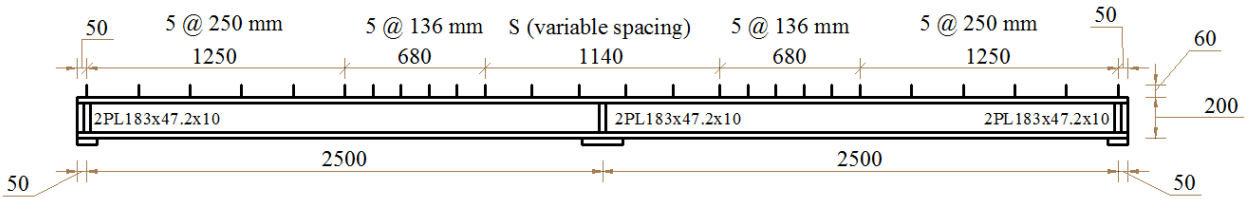

Figure 3.Spacing between Shear Studs at Sagging and Hogging Moment Zones

Table 1. Studs Spacing and Thickness of NC & UHPC at Hogging Moment of the Experimentally Tested Girders

Girder No.	Shear Stud Spacing (mm)			Thickness at Hogging moment (mm)	
	Sagging Moment		Hogging Moment		
	Mid-span to Exterior Support	Mid-span to Inflection Point		UHPC	NC
G1	250	136	127	0	90
G2	250	136	127	90	0
G3	250	136	127	45	45
G4	250	136	228	90	0

Table 2. Mechanical Properties of NC & UHPC

Mechanical Property	NC	UHPC
Compressive Strength (MPa)	25	134
Poisson's Ratio (□)	0.17	0.16
Young's Modulus (MPa)	20283	47,000
Flexural strength (MPa)	4.84	31

Table 3. Mechanical Properties of Steel

Mechanical Property	I-Beam	Rebar
Yield Strength (MPa)	306	555
Poisson's Ratio (□)	0.27	0.3
Young's Modulus (GPa)	193	171

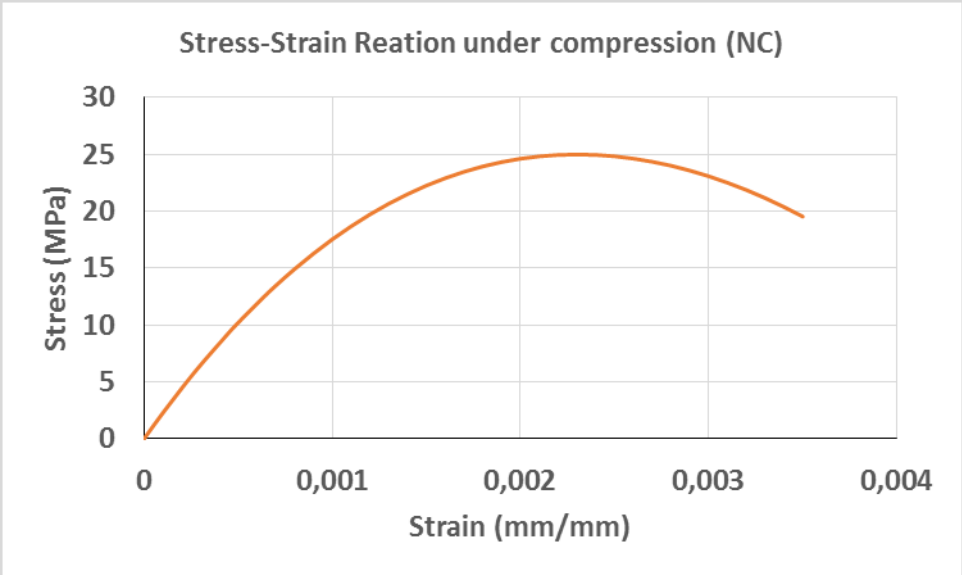

Figure 4. Stress-strain of NC under Compression

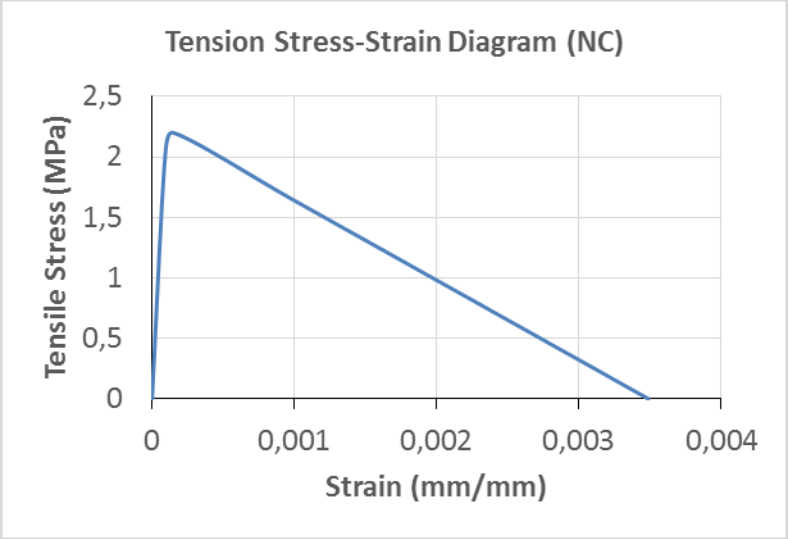

Figure 5. Stress-strain of NC under Tension

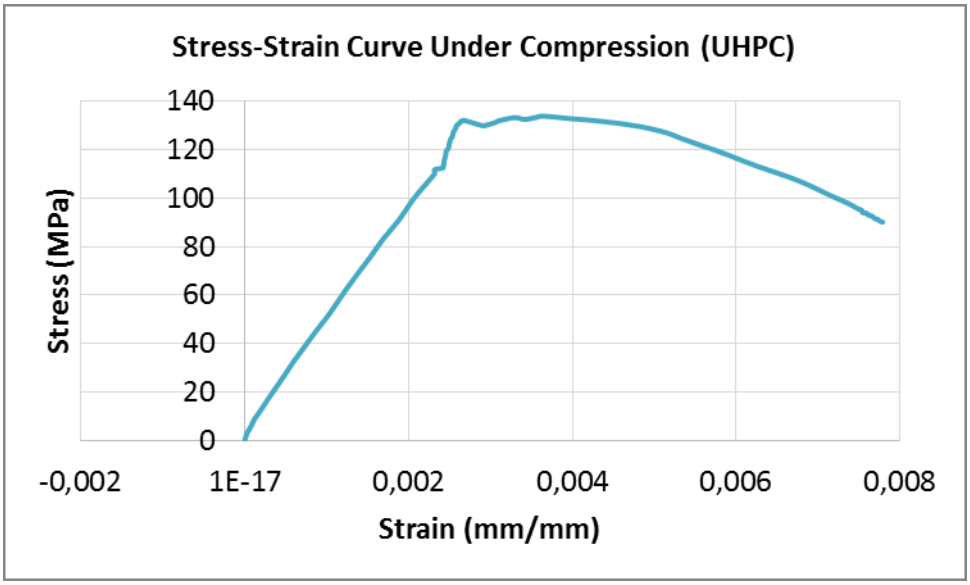

Figure 6. Stress-strain of UHPC under Compression

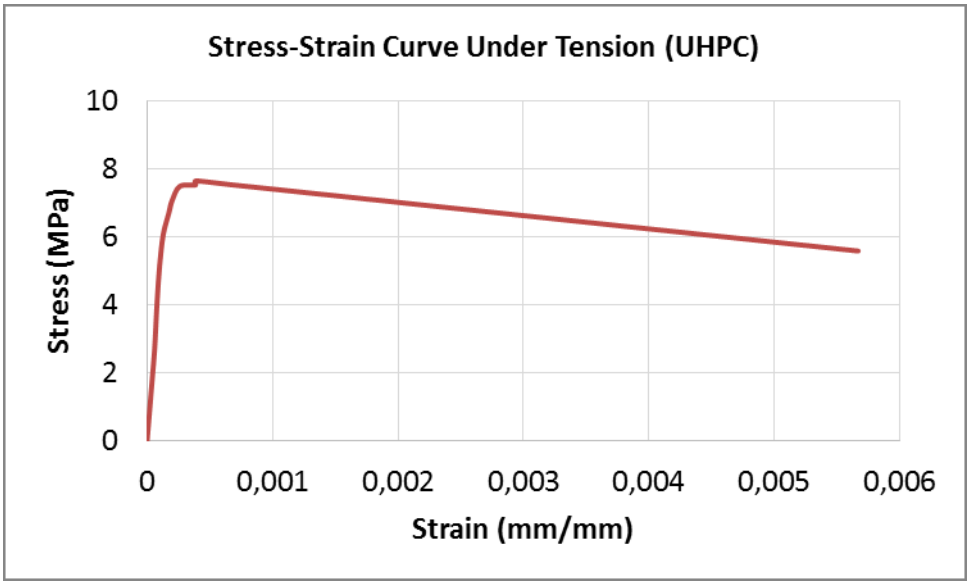

Figure 7. Stress- Strain of UHPC under Tension

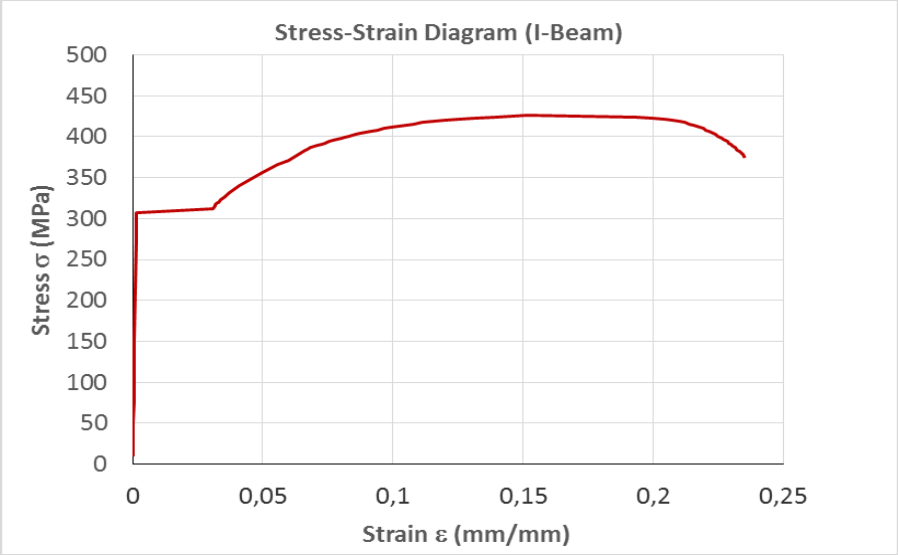

Figure 8. Stress-strain of Steel Section

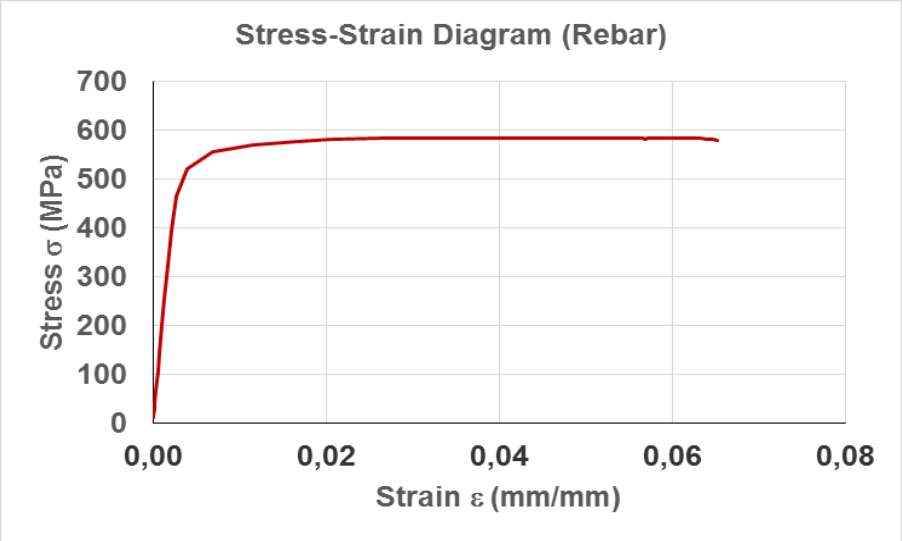

Figure 9. Stress-strain of Rebar

Finite Element Modeling

A 3D FE model of the continuous composite girders with UHPC slab at hogging moment zone was developed utilizing ABAQUS software [12]. The developed model includes material and geometrical nonlinearities. The model was validated with the obtained experimental results [12]. The suitable mesh and interface contact were used to predict the actual behavior of the composite girders. The verified model was employed to conduct a parametric study on the effect of the length of UHPC slab at hogging moment zone.

Modeling of Continuous Composite Girders with UHPC Slab

The brief description of FE modeling of continuous composite girders with UHPC slab at hogging moment zone is presented in this section.

Geometry and Elements Types

The continuous composite girder is composed of different components such as NC slab, UHPC slab, I-beam, reinforcement bars, transverse stiffeners, bearing plates over supports and under the applied load, and shear

studs. Those components were modeled as 3-D solid elements with their actual size except the reinforcements which were modeled as truss elements. Steel plates were used under the applied load to avoid stress concentration in the NC slab. All components were assembled together to form the complete continuous composite girder shown in Figure 10.

Two element types were used in the modeling of girders. Eight-node linear brick element (C3D8R) was used to model the solid elements. Two-node linear 3-D truss (T3D2) element was used for the longitudinal and transverse slab reinforcements.

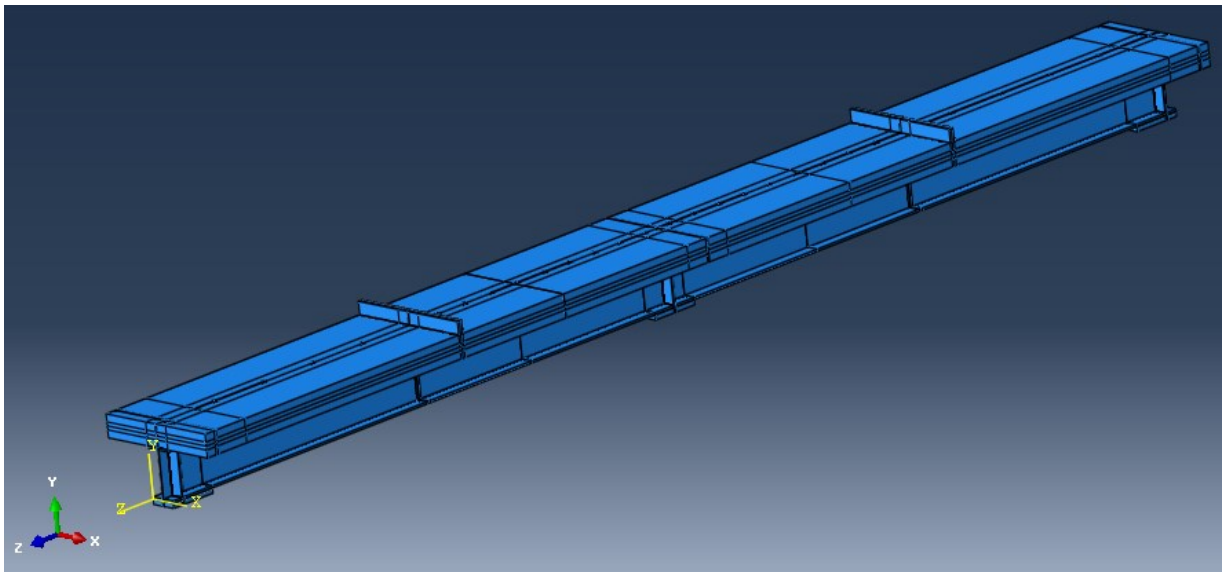

Figure 10. The Developed 3D FE Model

Materials Modeling

The assembled continuous composite girders are composed of different parts of different material properties such as NC, UHPC, slab reinforcements, and structural steel. Material models are explained briefly in the following subsections.

NC and UHPC

The behavior of NC and UHPC under compression was modeled as a nonlinear behavior. They were modeled as elastic-plastic materials including strain hardening part to predict the actual behavior of the composite girders accurately. NC and UHPC were modeled utilizing concrete damaged plasticity model (CDP) which was proposed by Lubliner et al. (1989) [19]. CDP is powerful model capable of predicting the behavior of concrete under both static and dynamic loading. The input parameters of CDP model are shown in Table 4.

Table 4. Input Parameters of CDP Model

	Density	Young's Modulus	Poisson's Ratio	Dilatation Angle	Eccentricity	F_{bo}/f_{co}	K	Viscosity parameter
NC	2.45E-6	20283	0.199	36	0.1	1.16	0.67	0
UHPC	2.50E-6	47000	0.16	36	0.1	1.16	0.67	0

Full stress-strain curves for NC and UHPC are shown in Figure 4 to Figure 7.The linear elastic part was modeled by the Young's modulus (E) and the Poisson's ratio (□). While, the nonlinear part is modeled by the stress-inelastic strain relation. In tension, the stress-strain relation increases linearly up to cracking stress and then decreases linearly.

Structural Steel and Rebar

Structural steel and steel reinforcements were modeled utilizing isotropic plasticity model. Steel was modeled as elastic-plastic material including material strain hardening. The elastic behavior was represented by the Young's modulus (E) and Poisson's ratio (□). While, the stress-strain curve was used to model the nonlinear/plastic

behavior. Table 3 shows the mechanical properties of different materials of steel. Figure 8 and Figure 9 show the stress versus strain relationship for structural steel and steel reinforcements, respectively.

Modeling of Contact Region

The assembled model contains many components which contact each other forming the interfacial zones. The interaction between the components was modeled using surface to surface contact. Different surface to surface models were used to simulate the interaction between reinforcements-concrete slab, shear connectors-concrete slab, shear connectors-steel beam, and stiffeners-steel beam. Tied contact was used to model the surface interaction between shear connectors and stiffeners with steel beam. It was used to simulate the perfect bond between contacted elements. The welded connections between steel beam with shear studs and transverse stiffeners are somewhat considered as perfect bond because failure in welding material was not possible to take place. For the contact between steel reinforcements and concrete slab, embedded contact was used to specify an element or a group of elements that lie embedded in a group of host elements whose response will be used to constrain the translational degrees of freedom of the embedded nodes (i.e., nodes of embedded elements). The reinforcements were modeled as the embedded elements while the concrete slab was the host region. Regarding the contact between shear studs and concrete slab, normal behavior and friction behavior models were used to simulate the contact between the different elements. Normal behavior with hard contact was used in the normal direction to avoid penetration of shear connectors into the concrete slab. While, friction behavior with 0.2-coefficient of friction was utilized in the tangential direction. Friction behavior is used at the interfacial regions where relative slip is possible to take place.

Model Meshing

Meshing of the assembled model is sensitive and requires special attention. The developed model was partitioned and discretized into small elements. Cell partitions was used to divide the irregular parts. Two element types were used in the modeling of girders. Eight-node linear brick element (C3D8R) was used to model the solid elements. Two-node linear 3-D truss (T3D2) element was used for the longitudinal and transverse slab reinforcements. Accuracy of the results depends upon the FE mesh. Therefore, different mesh sizes were tried prior to converging the final FE mesh which is shown in Figure 11.

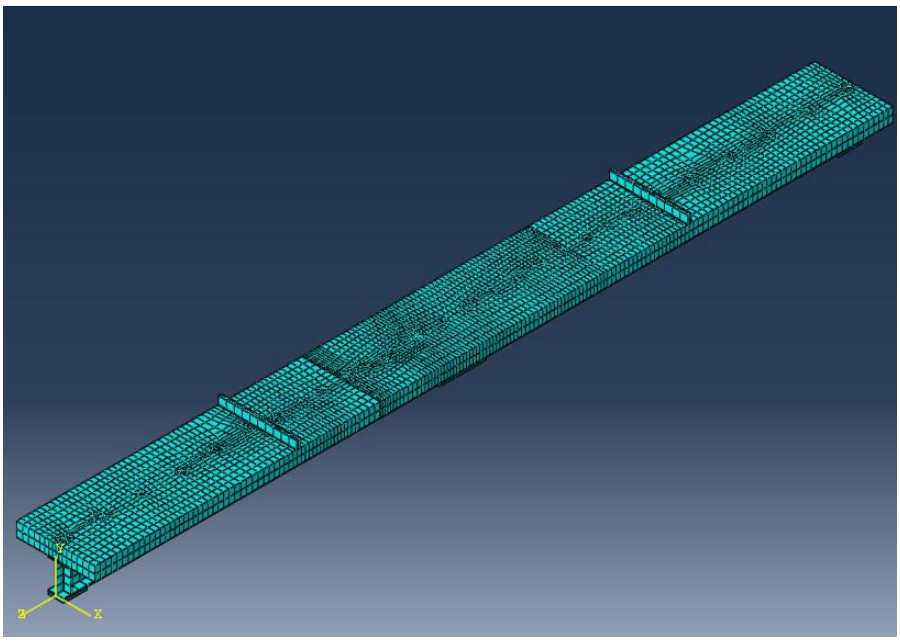

Figure 11. Meshing of the Composite Girder

Boundary Condition and Loading

The concentrated loading has been applied at the mid-span as an equivalent pressure over steel plates. The steel plates cover the full width of the concrete slab. Steel plates were used under the applied loads and over the

supports to avoid stress concentration in concrete slab and bottom flange of steel beam, respectively. Roller supports at both end of the specimen and rocker at the interior support were used to avoid rigid body motion. Figure 12 shows the applied loads at mid-spans and assigned supports.

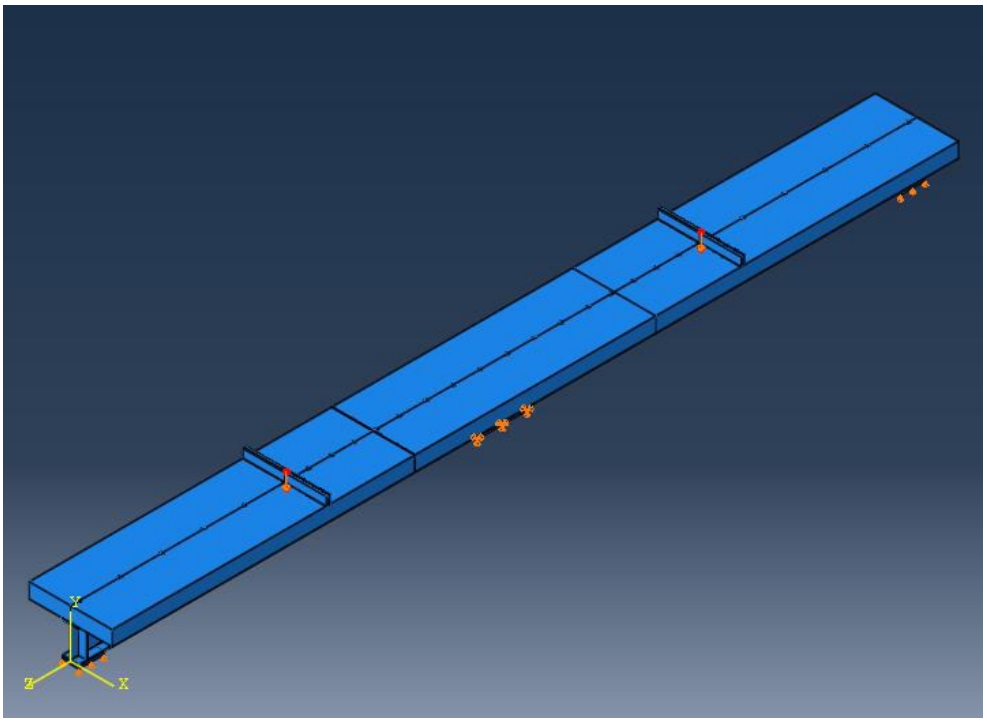

Figure 12. Assigned Boundary Conditions and Applied Load

Finite Element Validation

The developed model was validated against the conducted experimental data [12]. It showed a good agreement with experimental data. The comparison between the experimental and FE load-deflection curves for the four girders is shown in Figure 13 to Figure 16.Table 5 shows that the maximum percentage difference between the experimental and numerical ultimate loads is 3%. Shear-compression failure mode at the mid-span is observed as shown in Figure 18, NC reached the crushing strain leading to failure. The validated model can be extended to perform a parametric study to investigate the effects of the length og UHPC slab at hogging moment zone on the behavior of composite girders.

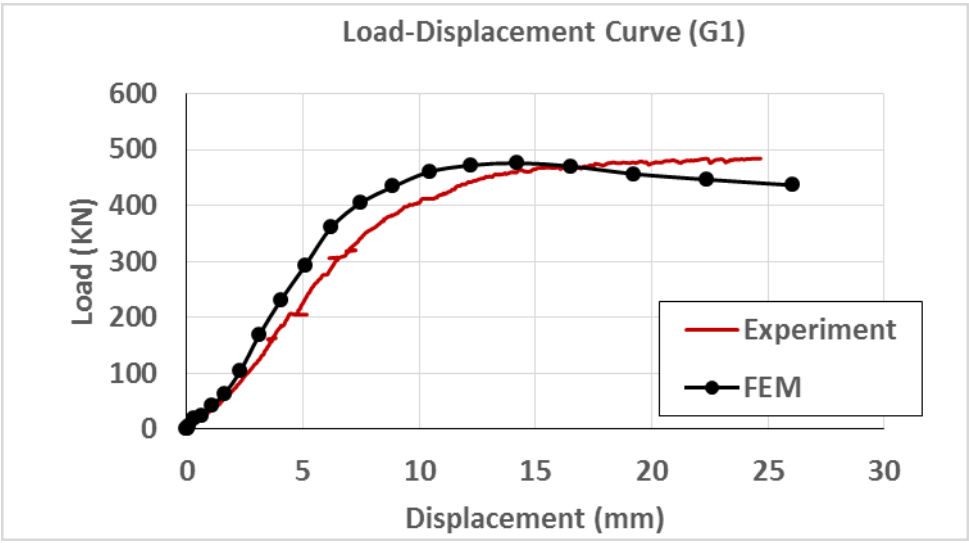

Figure 13. Load-displacement Curve for Girder G1

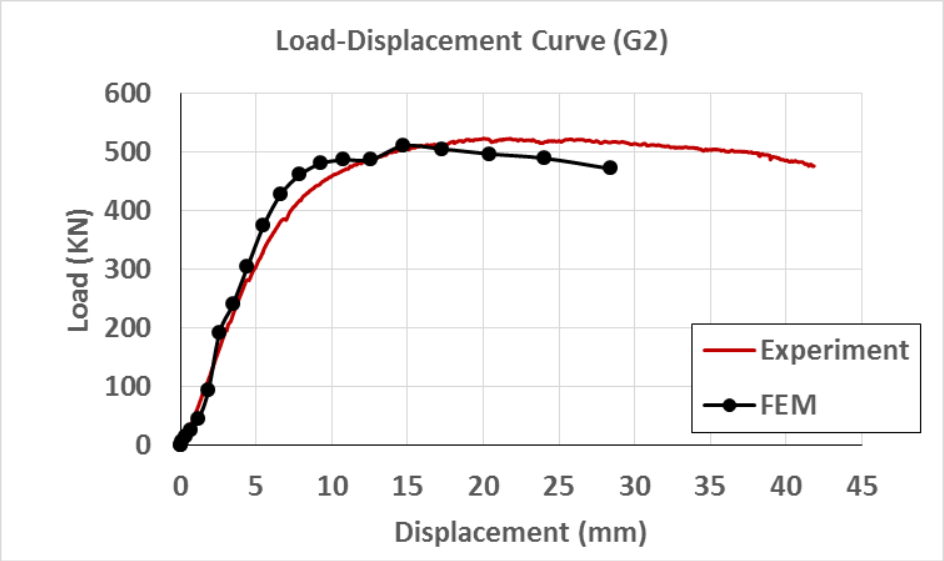

Figure 14. Load-displacement Curve for Girder G2

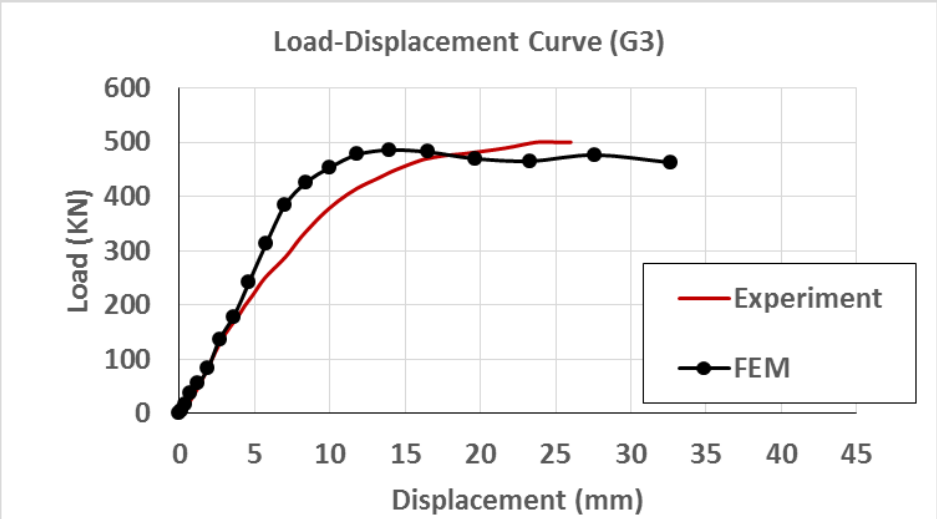

Figure 15. Load-displacement Curve for Girder G3

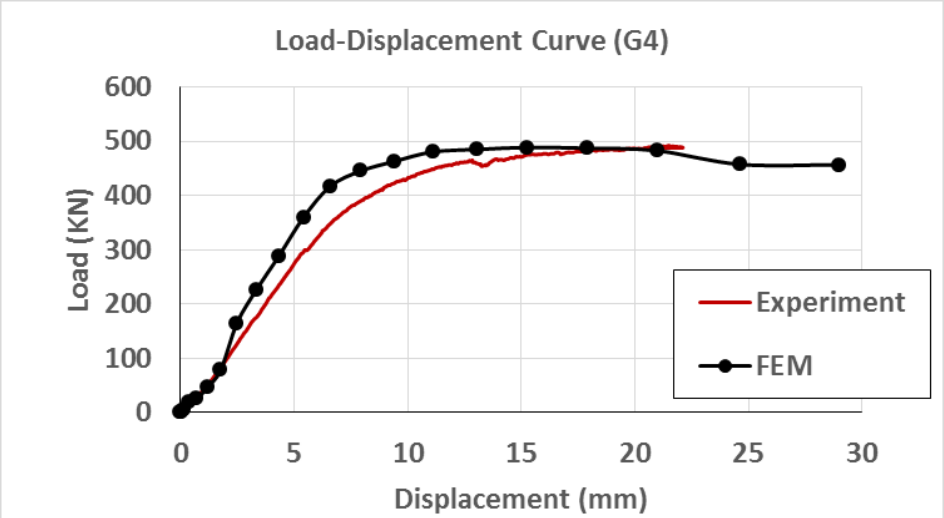

Figure 16. Load-displacement Curve for Girder G4

Table 5. Experimental and Numerical Ultimate Loads

Girder	Pu (Experiment)	Pu (Numerical)	Percentage Difference
G1	484	474	2%
G2	524	511.4	2%
G3	500	485	3%
G4	494	488	1%

Figure 17. Shear-compression Failure at Mid-span (Experimental)

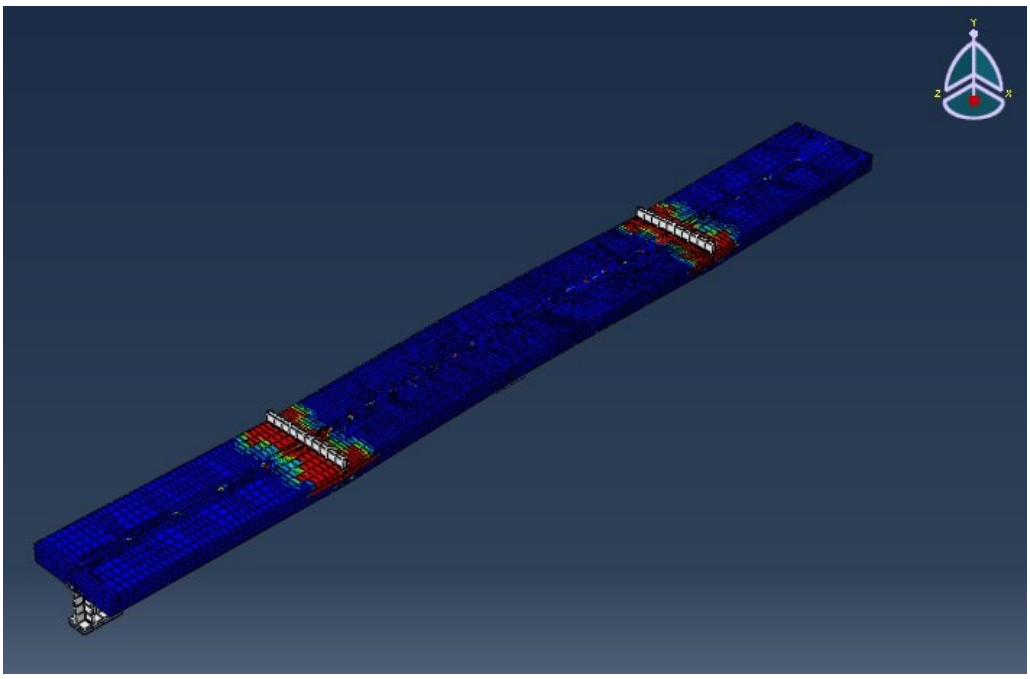

Figure 18. Shear-compression Failure at Mid-span (FE)

Parametric Study

Length of UHPC Slab

The effect of the UHPC slab length at hogging moment zone, shown in Figure 19, was investigated numerically utilizing ABAQUS software. A half-depth UHPC slab thickness and a 50%-degree of shear connection were implemented at hogging moment zone to evaluate the proper UHPC slab length that is sufficient for all loading conditions. This study considers symmetrical and unsymmetrical loading conditions to evaluate the critical UHPC slab length necessary to maintain the composite action at hogging moment zone.

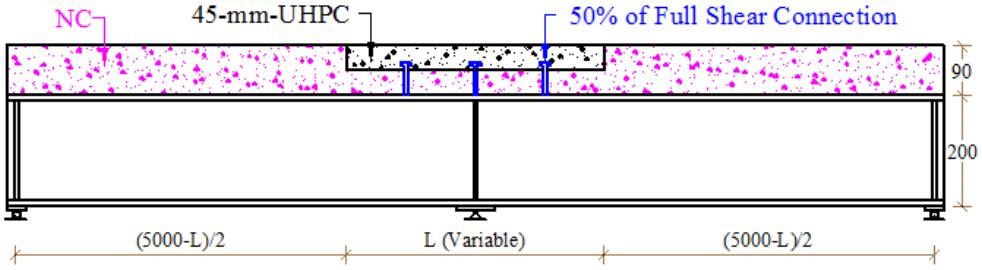

Figure 19. Varying the UHPC Slab Length at Hogging Moment Zone

The adequacy of the 1400-mm-length of UHPC slab to maintain the composite action at hogging moment zone was investigated for the symmetrical and unsymmetrical loading conditions shown in Figure 20 and Figure 21, respectively. These loading conditions are the most critical ones that require the largest length of UHPC slab. The results, summarized in Table 6, have shown that □□values are higher than one for all cases of loading, which indicate that the 1400-mm length is sufficient to maintain the composite action at hogging moment zone. Also, it is clearly shown that the symmetrical loading case 1, shown in Figure 20, is more critical than case 2 because it has a smaller value of □.

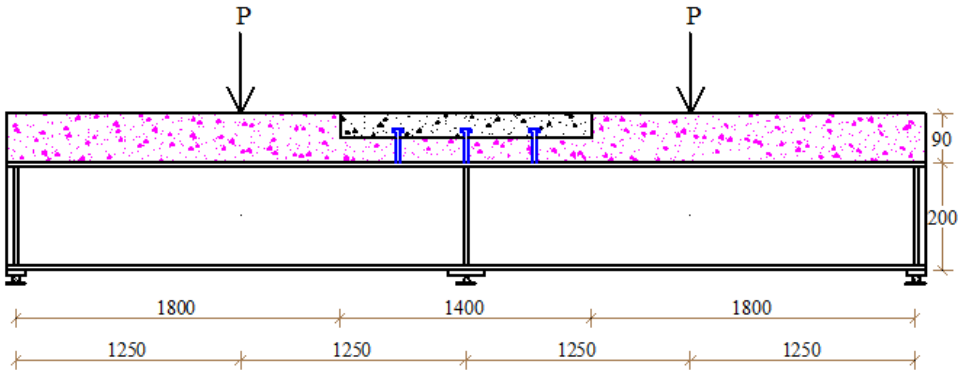

All dimensions are in (mm)

(a) Case 1: Two-point Loads applied at the Mid of Each Spa.

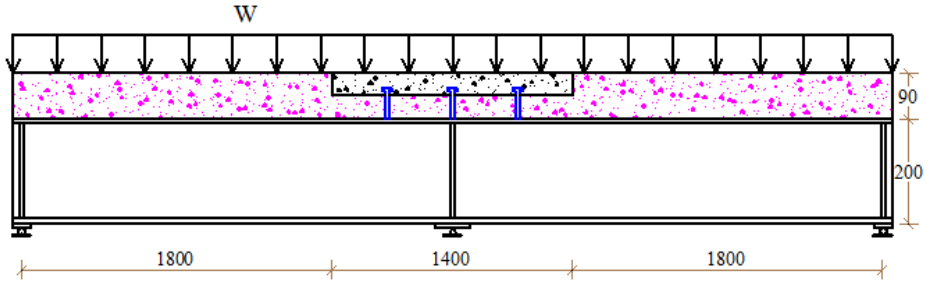

(b) Case 2: Uniformly Distributed Load Applied on the Two Spans.

Figure 20. Symmetrical Loading Conditions: (a) Case 1; (b) Case 2

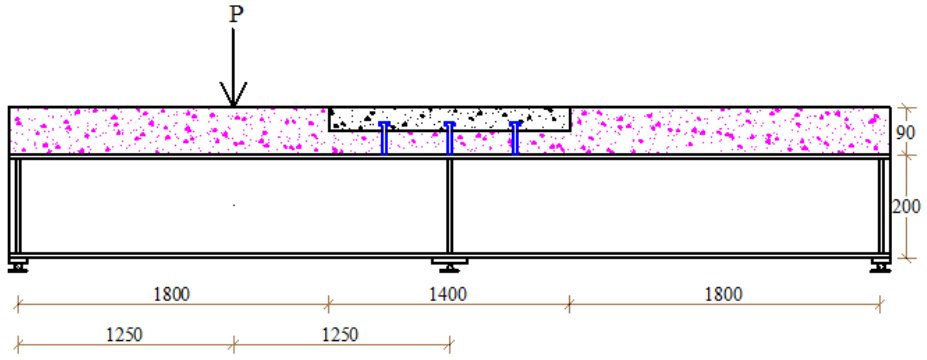

All dimensions are in (mm)

Figure 21. Unsymmetrical Loading Condition, Case 3

Table 6. Cracking, Yielding and □ Parameter for the Three-critical Cases of Loading

Loading Condition	UHPC Slab Length (mm)	Degree of Shear Connection	P_{cr} (kN)	P_y (kN)	□
Case 1	1400	50%	180	163	1.11
Case 2	1400	50%	1290	992	1.30
Case 3	1400	50%	228	202	1.13

Besides, the effect of the variable UHPC slab length, shown in Figure 19, was investigated numerically utilizing ABAQUS software for the most critical case of loading shown in Figure 21. Six girders (G-L0, G-L300, G-L600, G-L900, G-L1200 and G-L1500) were considered to evaluate the critical length of the UHPC slab at the hogging moment zone, as shown in Table 5.

Table 7. Varying the Length of UHPC Slab at Hogging Moment Zone

Girder	UHPC Slab Length (mm)
G-L0	0 (Only NC)
G-L300	300
G-L600	600
G-L900	900
G-L1200	1200
G-L1500	1500

The overall behavior of the composite girders with different UHPC slab lengths at hogging moment zone is illustrated by load-deflection curves, as shown in Figure 22. It is demonstrated that the length of UHPC slab slightly affects the ultimate capacity and stiffness of the composite girders, as shown in Figure 22 and Table.Also, insignificant variation in yielding load was obtained, as summarized in Table8. However, significant enhancement in cracking loads was obtained as increasing the length of UHPC slab, as shown in Table. Also, it is noticed that cracks initiated in NC slab for girders (G-L0, G-L300 and G-L600) and in UHPC slab for girders (G-L900, G-L1200 and G-L1500). The performance of girder G-L1500 with a 1500-mm UHPC slab length has not shown any improvement relative to the girder G-L1200, as shown in Figure 22 and Table8. While, it is clearly shown in Figure 22 and Table that as the UHPC slab length increases for girders (G-L900, G-L1200, G-L1400), their performance improved in terms of the stiffness, cracking load and □ values. Girder G-L900 with a UHPC slab lengthof900-mm gives a□ value close to one which represents a satisfactory UHPC slab length necessary to maintain the composite action at the hogging moment zone. Therefore, it can be concluded that the length of UHPC slab at hogging moment zone can be taken as 20% of the span length to achieve the desired performance of the continuous composite girders.

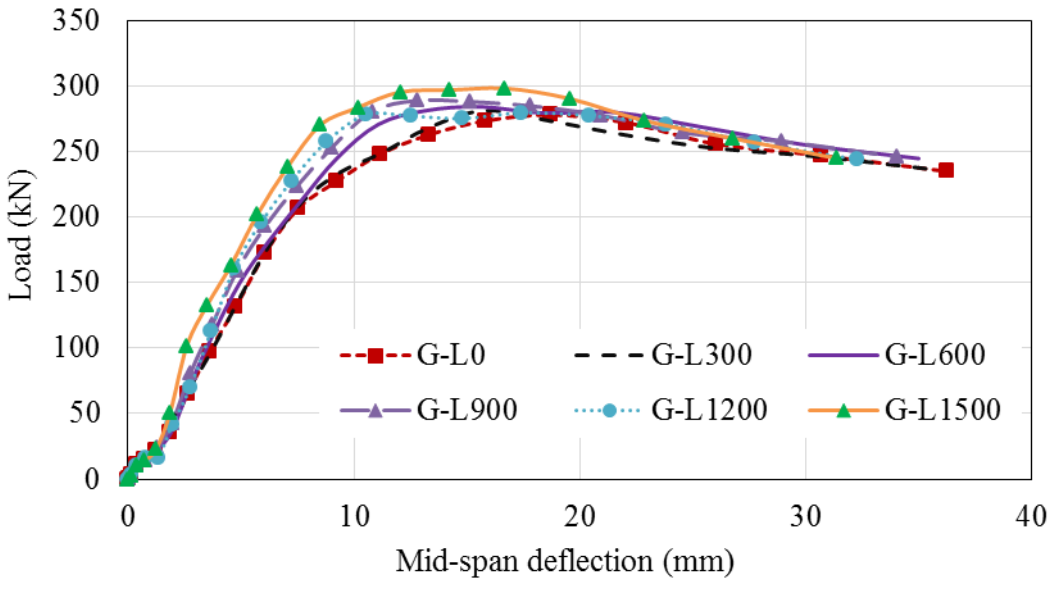

Figure 22. Load-displacement Curves for Girders with Different UHPC Length at Hogging Moment Zone

Table 8. Cracking, Yielding and Ultimate Loads Corresponding to Different UHPC Length at Hogging Moment Zone

Girder	UHPC Slab Length (mm)	Cracking of Concrete		Yielding of Steel			P_u (kN)
		P_{cr} (kN)	Location	P_y (kN)	Location		
G-L0	0 (NC)	147		175		0.84	278.1
G-L300	300	155	NC	178		0.87	281.4
G-L600	600	166		182	Bottom flange at mid-span	0.91	284.4
G-L900	**900**	**197**		**184**		**1.07**	**289.0**
G-L1200	1200	228	UHPC	186		1.23	297.5
G-L1500	1500	238		202		1.18	298.3

Conclusions

Four FE models were developed and investigated numerically utilizing ABAQUS software. The four models were validated against experimental results obtained from literature. Parametric study was performed to investigate the effect of the length of UHPC slab at hogging moment zone on the behavior of continuous composite girders. Based on the FE investigation, followings can be concluded:

- The use of a UHPC slab at the hogging moment zone maintained the composite action at a load level much higher than the upper service load limit and greatly improved the stiffness leading to a reduction in mid-span deflection;
- The ultimate load carrying capacity is slightly affected with the variation in the length of UHPC at the hogging moment zone;
- Cracking load is significantly improved with the use of UHPC at hogging zone. Steel fibers provide a post-cracking tension resistance which resist the initiation and propagation of cracks;
- The maximum service load is governed by yielding of steel beam rather than cracking of UHPC at hogging zone;
- The length of UHPC slab at hogging moment zone can be taken as 20% of the span length to achieve the desired performance of the continuous composite girders.

References

[1] American institute of steel construction (AISC) (2005). Manual, 13th Ed., Chicago.

[2] P. K. Basu, A. M. Sharif, and N. U. Ahmed, “Partially Prestressed Continuous Composite Beams. I”, Journal of Structural Engineering, 1987, 113, pp. 1909-1925.

[3] P. K. Basu, A. M. Sharif, and N. U. Ahmed, “Partially prestressed composite beams. II," Journal of Structural Engineering, 1987, 113, pp. 1926-1938.

[4] A. Elremaily and S. Yehia, “Use of External Prestressing to Improve Load Capacity of Continuous Composite Steel Girders”, ASCE Structures Congress, St. Louis, 2006.

[5] S. Chen, X. Wang, and Y. Jia, “A comparative study of continuous steel-concrete composite beams prestressed with external tendons: Experimental investigation”, Journal of Constructional Steel Research, 2009, 65, pp. 1480-1489.

[6] J. Nie, M. Tao, and S. Li, “Analytical and Numerical Modeling of Prestressed Continuous Steel-Concrete Composite Beams”, Journal of Structural Engineering, 2011, 137(12), pp. 1405-1418.

[7] A. Sharif, M. Samaaneh, A.K. Azad and M. Baluch, “Use of CFRP to maintaining Composite Action for Continuous Composite Steel-Concrete Girders”, Journal of Composite for Construction, 10.1061(ASCE) CC1943-5614.0000645, 2016, pp. 04015088(1-10).

[8] M. Samaaneh, A. Sharif, M. Baluch, and A.K. Azad, “Numerical Investigation of Continuous Composite Girders Strengthened with CFRP”, Steel and Composite Structures, International Journal, 2016, 21(6), pp. 1307-1325.

[9] Weiwei Lin, Teruhiko Yoda, Nozomu Taniguchi, Hideyuki Kasano, and Jun He. “Mechanical Performance of Steel-Concrete Composite Beams Subjected to a Hogging Moment”, Journal of Structural Engineering, 2014.

[10] Weiwei Lin and Teruhiko Yoda, "Experimental And Numerical Study on Mechanical Behavior of Composite Girders Under Hogging Moment", Advanced Steel Construction Vol. 9, No. 4, pp. 309-333 (2013).
[11] AASHTO LRFD Bridge Design Specifications. Washington, D.C.: American Association of State Highway and Transportation Officials, 2008.
[12] Sharifa AM, Assi NA, Al-Osta MA. Use of UHPC slab for continuous composite steel-concrete girders. Steel and Composite Structures. 2020 Jan 1;34(3):321.
[13] ABAQUS version 6.13-1 [Computer software]. Dassault Systèmes, Waltham, MA.
[14] Standard, A., ASTM C39 Standard Test Method for Compressive Strength of Cylindrical Concrete Specimens. ASTM International, 2015.
[15] ASTM C293, Standard Test Method for Flexural Strength of Concrete, ASTM International, West Conshohocken, PA, 2016.
[16] ASTM E8M-04, Standard Test Methods for Tension Testing of Metallic Materials [Metric] (Withdrawn 2008), ASTM International, West Conshohocken, PA, 2008.
[17] Hakeem, I.Y.A., "Characterization of an ultra-high performance concrete", King Fahd University of Petroleum & Minerals (Saudi Arabia), MSc Thesis, 2011.
[18] Eurocode-4. (2005). Design of composite steel and concrete structures - Part 1-1: General rules and rules for buildings (Vol. EN 1994-1-1). Brussels.
[19] Lubliner, J., Oliver, J., Oller, S. and Onate, E. (1989), "A plastic-damage model for concrete", Int. J. Solid. Struct., 25(3), 299-326.